Surface & Coatings Technology 204 (2010) 3954–3961

Contents lists available at ScienceDirect

Surface & Coatings Technology

journal homepage: www.elsevier.com/locate/surfcoat

Effect of polyethylene glycol on hydrophilic TiO_2 films: Porosity-driven superhydrophilicity

Weixin Huang, Ming Lei, Hong Huang *, Junchi Chen, Huanqin Chen

Guangdong Provincial Key Lab for Green Chemical Product Technology, South China University of Technology, Guangzhou 510640, PR China

ARTICLE INFO

Article history:
Received 21 September 2009
Accepted in revised form 18 March 2010
Available online 31 March 2010

Keywords:
TiO_2 film
Polyethylene glycol (PEG)
Cassie impregnating wetting regime
Superhydrophilic

ABSTRACT

Polyethylene glycol (PEG) 2000 was used as a templating reagent to synthesize porous TiO_2 thin film by sol–gel process. The nanopores resulting from the presence of growing cracks were ultimately formed on the surface when PEG content was higher than the critical value. Surprisingly, stable pore structure disappeared and surface became fluctuating and dehiscent after PEG amount increased to 0.02 M. Besides, two main hypotheses were proposed in order to explain this superhydrophilic behavior, namely the Wenzel and Cassie wetting impregnating models. Furthermore, the transition between these two wetting regimes was investigated and the criteria for the design and construction of Cassie impregnating wetting surface was also discussed. It was found that Cassie state shifting from Wenzel state could be easily achieved with increasing hole depth on TiO_2 surface. The study of transition between Wenzel and Cassie impregnating wetting regimes on porous films provides valuable wetting mechanism of porosity-driven wettability for the design of superhydrophilic surfaces.

1. Introduction

Hydrophilic surfaces have considerably technological applications due to their special properties [1–7]. Such materials are already commercialized as door mirrors for cars, coatings for buildings, self-cleaning glass, etc. TiO_2 is a widely used photocatalytic and hydrophilic material, which has been employed in many promising industrial applications for its fine optical, chemical and hydrophilic properties. Notwithstanding this trend, pure TiO_2 is limited for superhydrophilic application owing to its alternative photo-induced efficiency with light changes [8–10]. Recently, special attention has been focused on the structure modification of TiO_2 to permit its chemical composition and the topography of surface layers to improve hydrophilic performance [11–16]. It is generally believed that the use of a high-surface area, i.e., hierarchical or porous surface structure, rather than a commercially low surface area has some beneficial effects on hydrophilic behavior.

As most previous experiments, the natural tendency of solid is enhanced by the presence of a texture, which can make the apparent contact angles usually measured become different from those predicted by the Young equation [11,14,16,17]. The earliest works on this problem can be attributed to Wenzel and Cassie [18,19]. Their expressions, which were called Wenzel regime and Cassie–Baxter regime for the apparent contact angle, were based on certain average characteristics of the roughness. In Wenzel regime, it is well established, for example, that for a given chemical composition, the increasing roughness of a surface can render it more hydrophobic or more hydrophilic. On the other hand, according to traditional Cassie model, either air or the test liquid can remain trapped below the drop, which also leads to a superhydrophobic or superhydrophilic behavior. Superhydrophobic behavior (Cassie–Baxter type; water droplet contact angle > 150° and low contact angle hysteresis) occurs when air becomes entrapped in the nanostructure: in this state which is called Cassie air trapping regime, water droplets simply roll on the surface. On the opposite side, near complete wetting can occur if the structure of surface is readily invaded by water and can accommodate the full volume of the liquid droplet (Cassie impregnating wetting regime [20,21]; water droplet contact angle < 5° within 0.5 s or less). Additionally, the transition of different wetting regimes was subjected to intensive theoretical and experimental research recently [22–26]. Nevertheless, previous experiments are not conclusive regarding which regime to interpret the porosity-driven superhydrophilic state and the transition mechanism between these two superhydrophilic regimes has not been reported yet.

For the past few years, TiO_2 nanostructured films/arrays can be normally obtained through modified sol–gel routes in the presence of templates [27–32]. Among those templates, polyethylene glycol (PEG) is a traditional pore-forming one commonly used for the synthesis of porous TiO_2 thin films. It shows a long zigzag chain structure and extremely becomes a ring-network structure when it is dissolved in water or ethanol. We demonstrated that porous TiO_2 thin film doped with PEG was found to exhibit both antifogging and superhydrophilic although it was not exposed to ultraviolet irradiation due to its rough surface [33]. In this paper, the wetting on sol–gel derived porous films with different pores has been investigated. Two distinct hypotheses are classically proposed to explain this effect. A key finding of this work is that suitable wetting state must be chosen to interpret the formation of superhydrophilic TiO_2 thin film with porous structure.

* Corresponding author. Tel./fax: +86 020 87112047.
E-mail address: cehhuang@scut.edu.cn (H. Huang).

0257-8972/$ – see front matter © 2010 Elsevier B.V. All rights reserved.
doi:10.1016/j.surfcoat.2010.03.030

2. Experimental

2.1. Preparation of porous TiO_2 films

The special porous TiO_2 thin films were prepared by a sol–gel approach suitable for the different scale of pores using polyethylene glycol (PEG) as a pore-generating agent. The titania sol was prepared at room temperature in a classical method yielding a polymeric mother solution, which was obtained by mixing tetrabutyl titanate with deionized water, acetylacetone, hydrochloric acid, and absolute ethanol as a solvent. The concentration of tetrabutyl titanate in the solution was 0.5 M, and the Ti (OC_4H_9):EtOH:AcAc:H_2O:HCl molar composition was 1:60:0.5:2:0.1. To obtain different micro-nanostructured surfaces, different amounts of PEG (0.003, 0.006, 0.010, 0.012, 0.015 and 0.02 mol/L), which were named A1, A2, A3, A4, A5 and A6 respectively, were adopted in the mother solution for analyzing the hydrophilic conversion of the thin films with changing size of apertures. Meanwhile, in order to investigate the pore-forming process on TiO_2 surface, the following experimental situation was taken into consideration: the adding amount of PEG 2000 was controlled from 0.001 to 0.003 M. Finally, TiO_2 films were deposited by spin coating process from TiO_2 sols with different PEG concentrations onto glass substrates with the screw rotating rate of 800 rpm for 20 s and 3000 rpm for 10 s in succession. Then the coatings were dried at 100 °C for 0.5 h and calcined in air at 500 °C for 1 h using heating rate of 5 °C/min.

2.2. Characterizations

IR spectra were recorded on Vector 33 FTIR spectrometer from Bruker Corporation. Morphologies of the TiO_2 films were investigated by a LEO 1530 VP field emission-scanning electrons microscope (FE-SEM). Atomic force microscopy (AFM) measurement was performed using an instrument (CSPM 2003) with 3 μm × 3 μm scanned area and images were acquired under ambient conditions in contact mode using a Nanoprobe cantilever. Contact angles for water (WCA) were measured with an OCA40 contact angle goniometry from Dataphysics Co. Germany. Typically, the average value of five measurements, made at different positions of the film surface was adopted as the value of WCA.

The fraction of the liquid–solid interface in Cassie model was established with the image processing technique, i.e., it was supposed that the interface corresponds to the top parts among pores. The roughness parameter and hole depth were established from the Nanoscope system of atomic force microscope (AFM) for TiO_2 surfaces.

3. Results and discussion

3.1. FTIR spectra of sol process

The evolution of the infrared spectra is represented in Fig. 1 for different samples. The absorption of 3500–3000 cm^{-1} is due to stretching vibration of the hydroxyl groups in the titanium sol. By comparison of these traces, it can be seen that the bands in the 1400–1600 cm^{-1} range, characteristic of acetylacetonate groups bound to titanium, still remain intense during the hydrolysis process and polycondensation with PEG. The absorption peak from Ti–O–C (1097 cm^{-1}) disappeared when the mixture of water and EtOH was added into the solution, while it dramatically appeared after amounts of PEG were dissolved into the solution. This indicated that hydrolysis had occurred in the former solution and generated Ti–O–H bending, which was substituted by Ti–O–C bending during some polycondensations between PEG and the complexing products. Additionally, small colloidal particles were generated continually in the sol due to the stable hydrolysis of Ti $(OC_4H_9)_4$ and soon coated with PEG before polycondensation reaction.

3.2. Effect of PEG amount on morphological development of TiO_2 films

The micro-structured surface of TiO_2 thin films with different adding amount of PEG was studied. Fig. 2 shows the topography images of PEG-doped TiO_2 thin films heated at 500 °C (A1) with PEG 0.003 M, (A2) with PEG 0.006 M, (A3) with PEG 0.010 M and (A5) with PEG 0.015 M. In the figures, PEG-A1 gave the normally numerous nanopores with average size around 420 nm on the surface, a little smaller than those measured

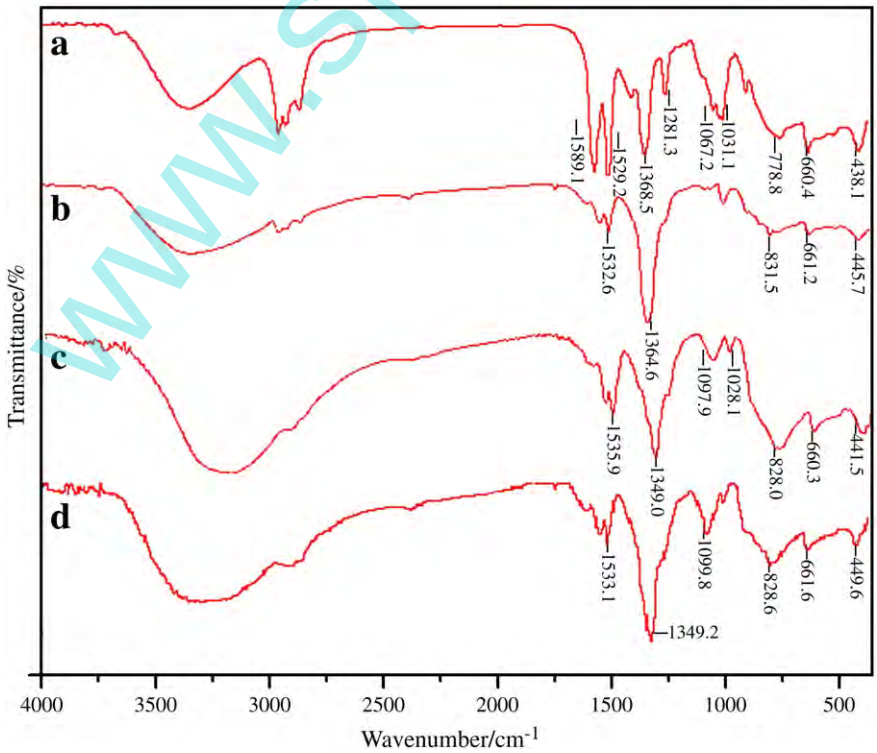

Fig. 1. FTIR spectra of titanium sol process: a—Ti$(OC_4H_9)_4$ + C_2H_5OH + AcAc; b—Ti$(OC_4H_9)_4$ + C_2H_5OH + AcAc + H_2O; c—titanium colloid + 0.003 M PEG; d—titanium colloid + 0.015 M PEG.

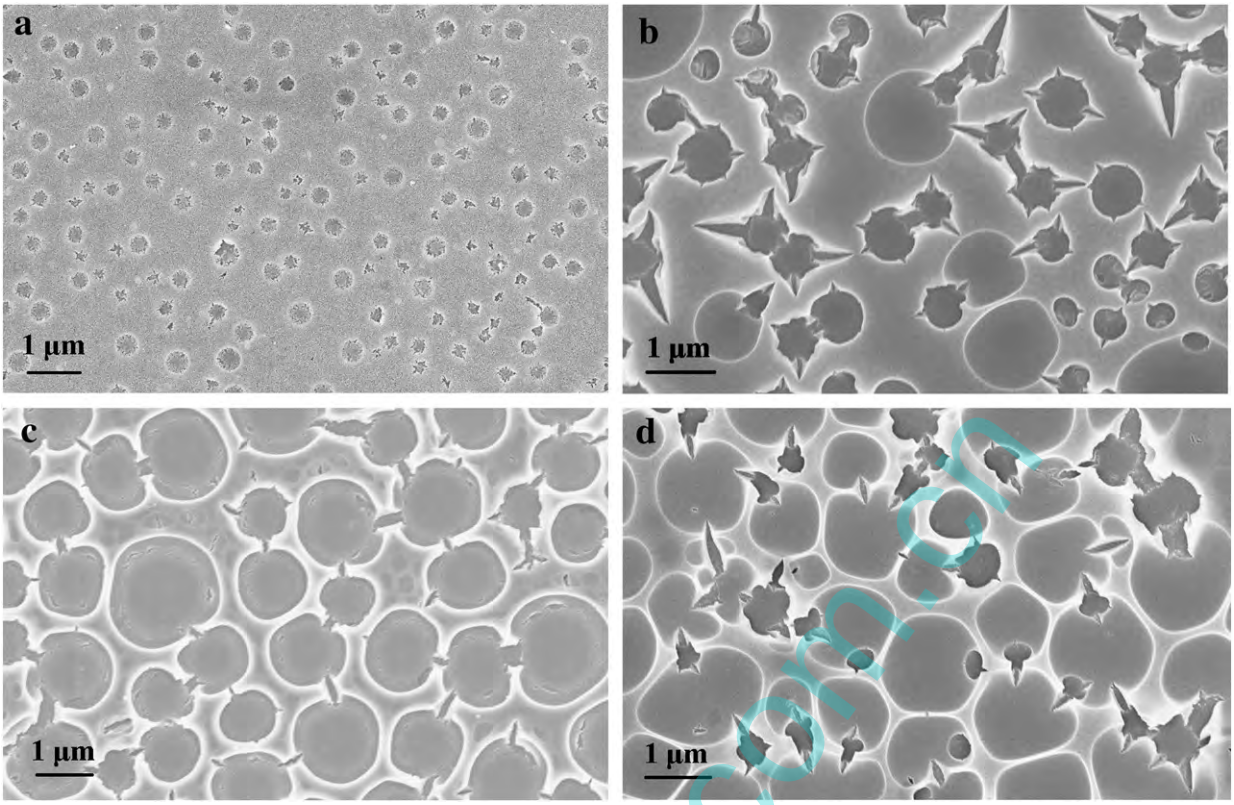

Fig. 2. FE-SEM images of PEG-doped TiO_2 (a) 0.003 M, (b) 0.006 M, (c) 0.010 M, and (d) 0.015 M.

on PEG-A2 sample and PEG-A3 sample, which were approximately 0.8 μm and 1.1 μm respectively after sintering. Comparatively, the total crystallization of flat TiO_2 coating with a narrow crystal size distribution can be prepared with no PEG treated in the same experimental condition [33]. Therefore, it could be considered that pores in these TiO_2 film made an upward trend in diameters and depths with the enhancing amount of PEG.

Meanwhile, it deserves to be mentioned that the pore-forming process was ascribed to the presence of PEG. Actually, the polyethylene glycol could oxidize and decompose to carbon dioxide which left numerous small cracks on the surface when its adding amount was 0.0025 M (see Fig. 3). Surprisingly, if the PEG amount was lower than 0.002 M (Fig. 4), small cracks on the surface would easily disappeared since TiO_2 grain size was enlarged in the TiO_2 film during thermal treatment. This indicated, as anticipated, that TiO_2 colloidal particles were absorbed on the same PEG chains (Fig. 5a) since PEG content in TiO_2 sols was lower than the critical value (0.002–0.0025 M), thus colloidal particles cannot be coated by PEG and serious agglomeration among particles occurs over the period of thermal treatment. In contrast, PEG molecules were absorbed on the same TiO_2 particle surface when the PEG amount was higher than the critical value (see Fig. 5b), and then TiO_2 colloidal particles did not easily agglomerate due to the steric hindrance of PEG molecular chains. According to Fig. 3, numerous small cracks were generated in randomly circular regions due to the linkage between Ti

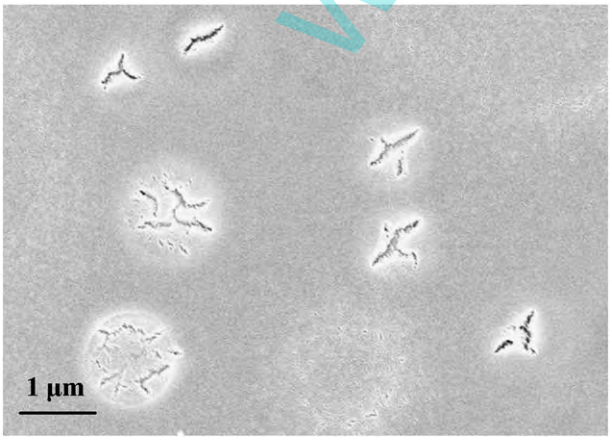

Fig. 3. FE-SEM images of numerous small cracks on TiO_2 surface.

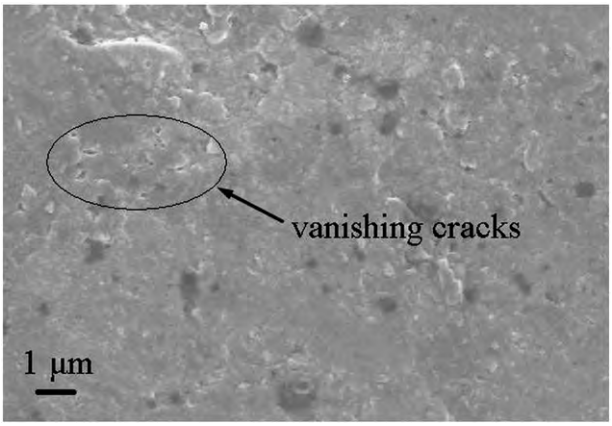

Fig. 4. Small vanishing cracks on TiO_2 surface after sintering.

Fig. 5. Effect of PEG amount on TiO_2 colloidal particles (a) lower than critical content and (b) higher than critical content.

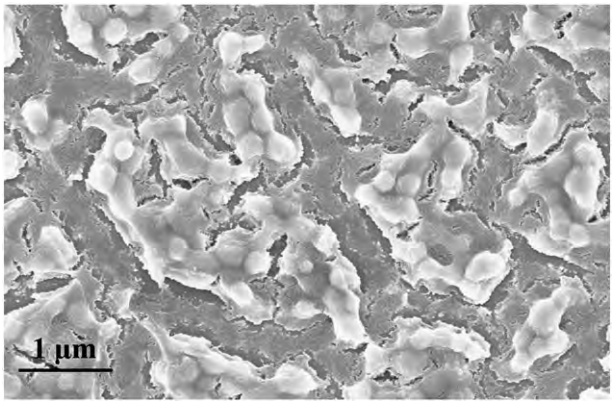

Fig. 6. Irregular and fluctuating PEG-doped TiO_2 surface (A6).

$(OH)_4$ particles and PEG, and it seems that increasing small cracks ultimately form pores, which increase the special surface area. Besides, we found out that a considerable amount of small holes occurred on the top surface among large holes as PEG content increased to 0.015 M (Fig. 2d). The formation of many small clusters among large clusters, which was attributed to CH_2–O…Ti bonding, induces the growth of these small holes. In this case, PEG molecules therefore would not contribute to a complete enlargement of aperture, and the shape of holes would become irregular and fluctuating as the content of PEG continued to increase to 0.02 M (sample A6), which was shown in Fig. 6. The reason is that the combination of PEG is stronger than complexing of Ti sol and PEG, and excess PEG can self-assemble and finally separate out in sol, which invalidates the mechanism of phase separation [34].

3.3. Wetting state: experimental data and their interpretation

Final apparent contact angles (θ_{fin}), corresponding to the wetting transition onset, can be measured on the above-mentioned substrates and listed in Table 1, together with calculated ones according to the well-known Wenzel (Eq. 1) and Cassie equation (Eq. 2). The same technique was used for the determination of contact angle on the flat TiO_2 surface (the Young angle).The initial (flat surface) and final (porous surface) wetting states are stable. It could be easily recognized that θ_{fin} is much smaller than θ_{flat}, and the decrease in final apparent contact angles was observed on surfaces A1–A5, but it was not observed on surface A6 where PEG amount was larger than 0.02 M. After doped PEG into the TiO_2 sols, they (surfaces A2–A5) undergo a wetting transition from hydrophilicity to superhydrophilicity. Since superhydrophilic behavior is only observed on PEG-doped films, it is reasonable to suggest that the addition of PEG was contributed to macro-nano pores that ultimately give rise to superhydrophilicity.

Following two different wetting regimes would be significantly discussed for the adaptation to the sudden growth in the hydrophilicity of the TiO_2 films. It has been reported that rough surface may change the contact angle, and that microtextured topography can also influence [15,16,35]. In many cases, it turns out that drops on textured materials are observed to be in the Wenzel regime and Cassie regime. It is firstly indispensable to suggest that the hydrophilic wetting states, namely the Wenzel state, can interpret the wetting transition from initial apparent contact angle of the flat surface to final apparent contact angles with nanoporous surfaces which were observed in these experiments. The Wenzel model describes homogeneous wetting by the equation [18]:

$$\cos\theta_w = r\cos\theta_0 \quad (1)$$

where θ_w and θ_0 are Wenzel contact angle and the Young's CA of a flat surface, respectively and r is the roughness factor, defined as the total surface area to the projected area in the horizontal plane.

In a hydrophilic surface ($\theta<\Pi/2$), Eq. (1) implies the solid roughness that makes the solid more wettable. Contact angle, for certain, can sharply decrease with the corresponding linear slope of the equation and easily become zero as PEG amount exceeding 0.003 M in the complete Wenzel state presented in the table. Identification of transitional and final wetting regime could be achieved from the comparison of the angles predicted by Eq. (1) with the experimental data summarized in Table 1. For surfaces A1–A5 which are 'too hydrophilic', a different law is followed, which also seems to be linear in this plot, yet with a slope smaller than the Wenzel one. This different behavior here indicates that the final wetting state for surfaces A1–A5 is not Wenzel regime as previously supposed.

Comparatively speaking, it was also demonstrated that at least one more wetting regime of hydrophilic exists on the textured surface, namely the Cassie impregnating wetting regime, which supposed that the mixed surface is comprised of solid and the text liquid [21]. Thus, this model describes heterogeneous wetting by the equation [19]:

$$\cos\theta_c = 1 - \varnothing_s + \varnothing_s\cos\theta_0 \quad (2)$$

where θ_c and θ_0 are the Cassie contact angle and the Young contact angle, respectively, and $\varnothing_s$ is the area fraction of dry solid "islands" in the mixed surface beyond the drop.

This model describes the penetration front spreads beyond the drop and a new solid–liquid film forms over the surface, which was displayed in Fig. 7. Proper understanding of the Gibbs energy and the energy barrier is also the key for studying hydrophilic properties of porous surfaces. The Wenzel and Cassie impregnating wetting regimes are sometimes treated as two-phase states with a certain energy barrier associated with the phase transition [20,36]. Fig. 8 shows the transition of Gibbs energy of a droplet on the micropatterned surface with certain chemical composition. In our experiments, the rough TiO_2 surfaces with different topography are composed of the same chemical component (anatase phase) after calcined at 500 °C [33]. Therefore, it was extremely instructive to study and explain the possibility of this above-mentioned

Table 1
Measured and calculated contact angles of samples corresponding to different wetting states.

Sample	The amount of PEG/(M)	Roughness, f	Wenzel, θ^{calc}_{Wenzel}	Fraction of SG interface, $\varnothing_s$	Liquid trapping Cassie, θ^{calc}_{Cassie}	Final apparent contact angle, θ_{fin}
Flat	0	1	–	1	–	16.12 ± 1[a]
A1	0.003	1.26	0	0.85	14.79	12.34 ± 2
A2	0.006	1.41	0	0.61	12.52	8.16 ± 2
A3	0.010	2.08	0	0.24	7.85	5.97 ± 3
A4	0.012	2.26	0	0.20	7.16	4.92 ± 2

[a] The Young angle on a flat TiO_2 surface.

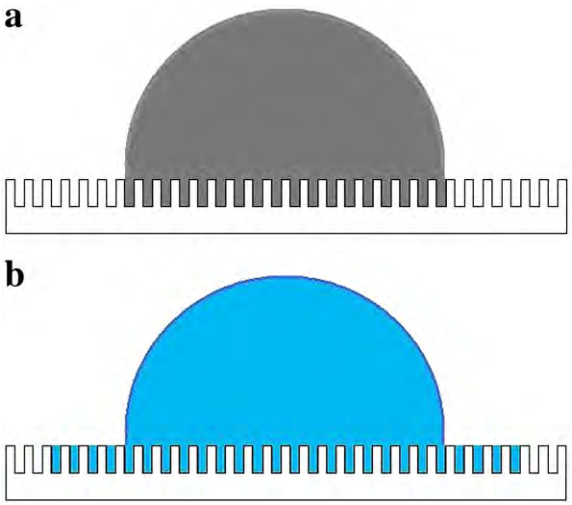

Fig. 7. Wenzel (a) wetting regimes and Cassie impregnating wetting regimes (b).

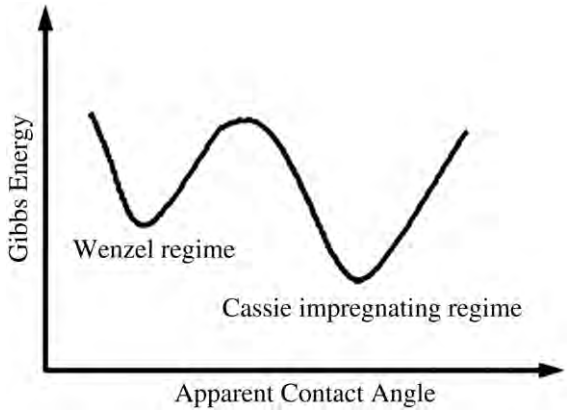

Fig. 8. Schematics of the Gibbs energy curve for wetting states: the Wenzel state and the Cassie impregnating wetting state.

surface structure-induced transition from Wenzel to Cassie impregnating regime on porous TiO_2 thin films. When a liquid film impregnates a texture ahead of the droplet from the Wenzel state, the corresponding change in interfacial Gibbs free energy writes:

$$\Delta G = (\gamma_{SL} - \gamma_{SG})\left[n\pi dh + n\pi\left(\frac{d}{2}\right)^2\right] + \gamma_{LG} n\pi\left(\frac{d}{2}\right)^2 \quad (3)$$

where γ, h and d are surface tension, hole depth and hole diameter, respectively. Associated with Young's relation, this yields:

$$\Delta G = \gamma_{LG} n\pi\left(\frac{d}{2}\right)^2 - \gamma_{LG}\left[n\pi dh + n\pi\left(\frac{d}{2}\right)^2\right]\cos\theta. \quad (4)$$

Here, the surface tension of liquid corresponded to the deionized water (fixing γ_{LG}, $\gamma_{LG} > 0$). Thus, the imbibition's front progresses occur only if the energy of the Cassie state should be lower than that of the Wenzel state, namely ΔG is negative. Eq. (4) can also be recasted in the following equation:

$$\cos\theta > \frac{d}{4h + d}. \quad (5)$$

Apparently, if Young's contact angle is larger than $\Pi/2$, the solid remains dry beyond the drop, and the Wenzel's relation Eq. (1) applies. On the other hand, a CA for the smooth resulting surface is between $\Pi/2$ and 0, thus the Cassie impregnating wetting regime should be metastable—a film develops in the texture and the drop sits upon a mixture of solid and liquid (Fig. 7b). According to formula (5), there clearly exists a gradual transition of the porous TiO_2 surface from Wenzel regime to Cassie impregnating wetting regime as the hole depth increases, and also the decrease in diameter with unchanged hole depth can also expand the propagation of water droplet into each of pores, which leads to a broadening of the front. More generally, formula (5) is also a criterion which shows the condition for the regime's transition ($\theta_c = \arccos\left(\frac{d}{4h + d}\right)$). The spreading occurs since the CA of the flat surface is smaller than the critical contact angle, θ_c. In this regard, the energy supplied by porous thin film in this case is sufficient for exceeding the potential barriers separating wetting states into Cassie impregnating wetting state.

The pore depths of A1 and A2 are 66.4 ± 10 nm and 82.8 ± 10 nm respectively, while the other three samples are 102 ± 18 nm. The corresponding diameters for the samples A1–A4 are about 0.4, 0.8, 1.1 and 1.2 μm, respectively. According to the measured water CAs of the prepared porous TiO_2 films shown in Table 1, the CA decreased slightly from 16° to 12° when small holes appeared in sample A1. For this porous substrate with a diameter of 0.4 μm and a hole depth of 66.4 ± 10 nm, the impregnating condition can be satisfied which indicates that the sample A1 was in the complete Cassie state. Besides, further increase in hole depth to 82.8 ± 10 nm raised the trend and resulted in the decrease in CA to 8.16°. When the holes became deeper (102 ± 18 nm), the CA remained essentially superhydrophilic. Therefore, if we apply the Cassie impregnating model developed for porous and heterogeneous surface, we can explain the observed experimental observation well.

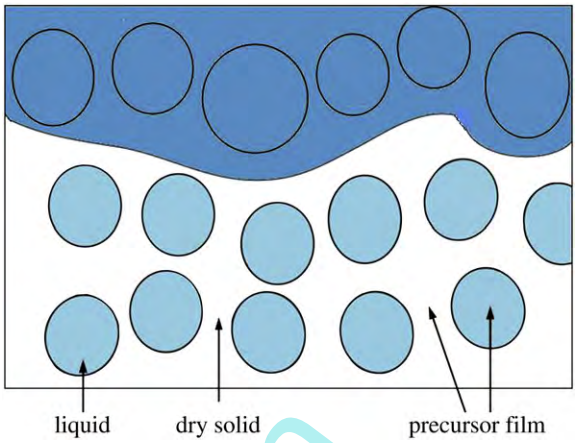

Fig. 9. Scheme illustrating the precursor film consisted of pores filled with liquid and dry solid.

It is noteworthy that as for the Cassie impregnating wetting discussed in this experimental situation, we should not consider these rough surfaces as homogeneous surface any more when a liquid film impregnates a texture ahead the drop, depicted in Fig. 9. The reason is that the gaps between the peaks were filled by another material (pores are filled with liquid) so that the "real" surface, on which a liquid drop was placed, consisted of two different materials. It therefore should be considered as heterogeneous surface. An additional consideration which supposing the drop is surrounded by a thin precursor film, may justify the success of the Cassie impregnating wetting regime [25,36,37]. Indeed at least partially liquid impregnating pores of the template could be seen through the thin water precursor film. The precursor film is adjacent to the drop boundary. It smoothes away local windings of the triple line and diminishes the energy excess connected with the triple line bending.

4. Conclusions

The mechanism for formation and superhydrophilic activity for porous TiO_2 thin film modified by polyethylene glycol (PEG) with average molecular weight 2000 was systematically investigated. It has been found that the amount of PEG as a pore-generating agent significantly affects microstructure and hydrophilic properties of the obtained TiO_2 nanoporous films. The appearance of small cracks on the surface was attributed to small clusters, consisted of PEG and TiO_2 particles, when the amount of PEG was higher than the critical value on the sol. The aperture and depth of pores showed a gradual rise with the enhancing amount of PEG. Furthermore, stable porous structure disappeared and the surface became fluctuating and dehiscent if PEG amount increased to 0.02 M. Besides, the wetting transition was observed between Wenzel and Cassie (impregnating) wetting states. The direct evidence for existence of the Cassie impregnating wetting regime upon wetting with rough surfaces can be obtained by the quantitative comparison and the regime's transition criterion $\left(\theta_c = \arccos\left(\frac{d}{4h + d}\right)\right)$. The wetting transition between Wenzel and Cassie impregnating wetting of the surfaces which is based on the multiple minima of Gibbs energy of droplet can be controlled by two major factors: the hole depth and diameter. If the hole depth increases, the wetting state will exhibit characteristics more like the Cassie impregnating state. What is more, the spreading of water in porous surface will occur if CA of the flat surface is smaller than critical contact angle, θ_c.

Appendix A

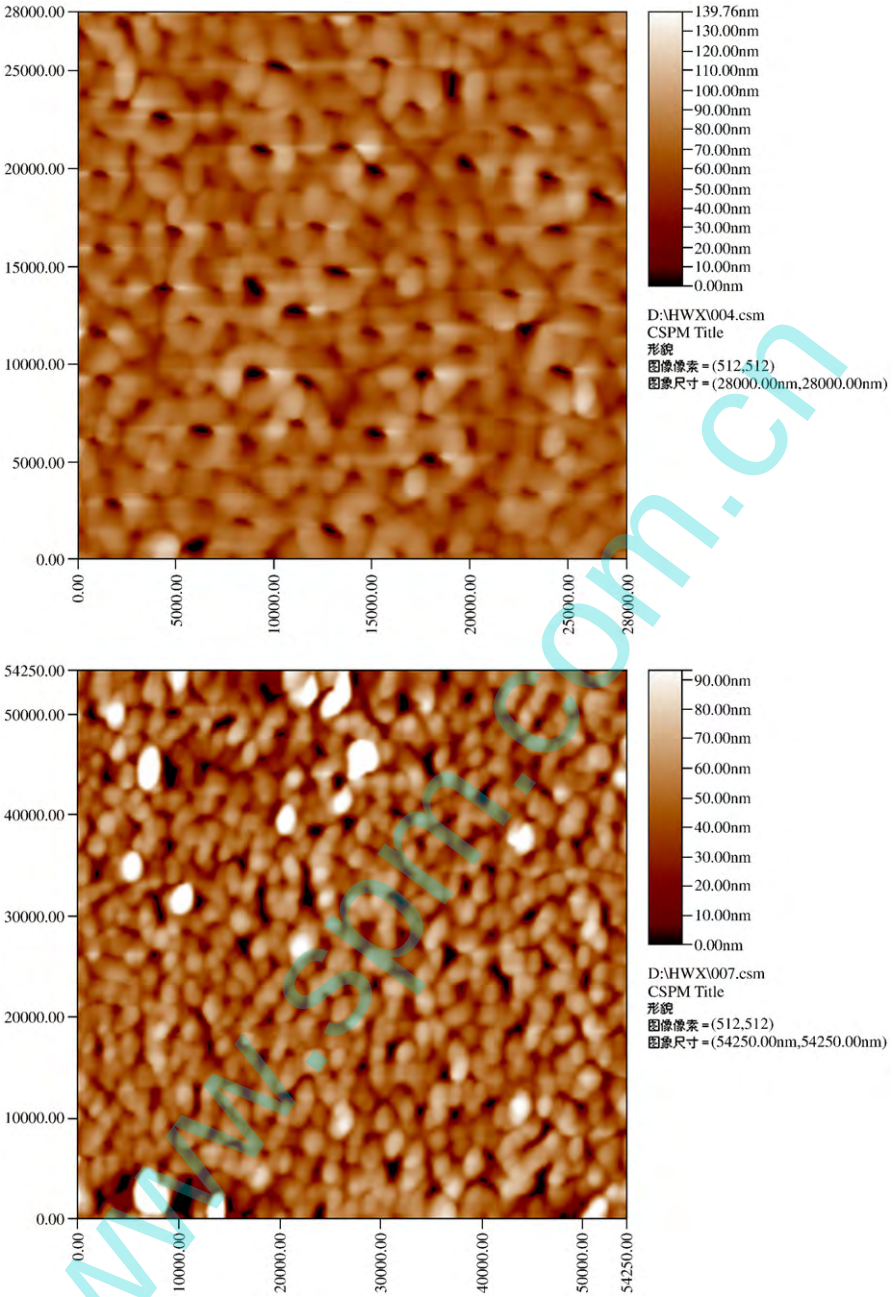

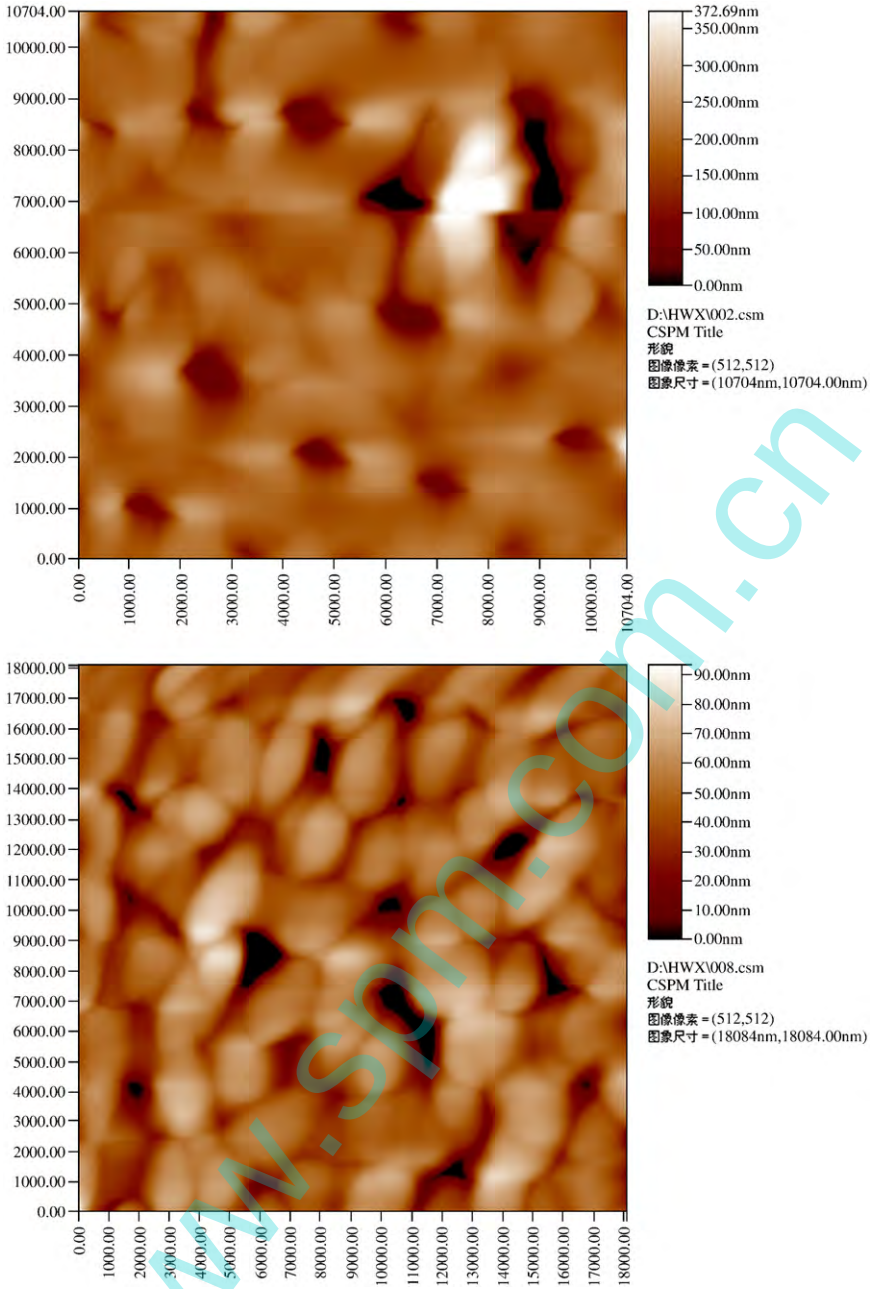

Fig. A. AFM images of PEG-doped TiO_2 (A1) 0.003 M, (A2) 0.006 M, (A3) 0.010 M, and (A4) 0.012 M.

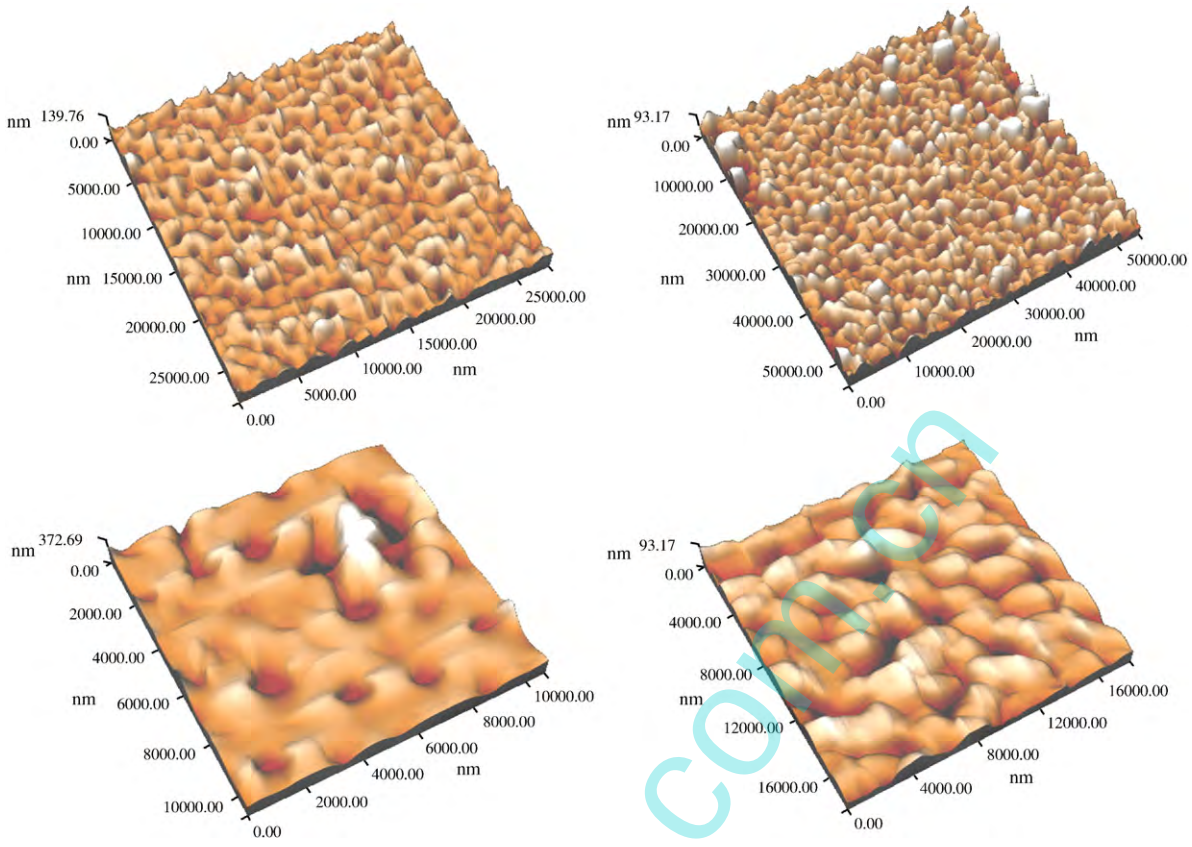

Fig. B. AFM 3D images of PEG-doped TiO_2 (A1) 0.003 M, (A2) 0.006 M, (A3) 0.010 M, and (A4) 0.012 M.

Table A1
The corresponding area–perimeter data of these surfaces.

Sample	Area (nm^2)	Perimeter (nm)
Flat	1.48e + 006	1.475e + 004
A1	1.095e + 008	1.096e + 005
A2	4.004e + 008	2.112e + 004
A3	9.227e + 006	4.454e + 004
A4	1.97e + 007	6.925e + 004

References

[1] J.B. Han, X. Wang, N. Wang, Z.H. Wei, G.P. Yu, Z.G. Zhou, Q.Q. Wang, Surf. Coat. Technol. 200 (2006) 4876.
[2] A. Chunder, K. Etcheverry, G. Londe, H.J. Cho, L. Zhai, Colloids Surf., A 333 (2009) 187.
[3] R.J. Sengwa, S. Choudhary, S. Sankhla, Colloids Surf., A 336 (2009) 79.
[4] N. Sakai, A. Fujishima, T. Watanabe, K. Hashimoto, J. Phys. Chem. B 107 (2003) 1028.
[5] T. Ishizaki, H. Sakurai, N. Saito, O. Takai, Surf. Coat. Technol. 202 (2008) 5535.
[6] Y. Suda, H. Kawasaki, T. Ueda, T. Ohshima, Thin Solid Films 453 (2004) 162.
[7] J.G. Yu, X.J. Zhao, Q.N. Zhao, Thin Solid Films 379 (2000) 7.
[8] E. Aubry, V. Demange, A. Billard, Surf. Coat. Technol. 202 (2008) 6120.
[9] A.A. Ashkarran, M.R. Mohammadizadeh, Mater. Res. Bull. 43 (2008) 522.
[10] P. Novotna, J. Zita, J. Krysa, V. Kalousek, J. Rathousky, Appl. Catal., B 79 (2008) 179.
[11] D.W. Jing, Y.J. Zhang, L.J. Guo, Chem. Phys. Lett. 415 (2005) 74.
[12] T. Sreethawong, S. Yoshikawa, Int. J. Hydrogen Energy 31 (2006) 786.
[13] T. Sreethawong, S. Laehsalee, S. Chavadej, Catal. Commun. 10 (2009) 538.
[14] D. Crisan, et al., J. Phys. Chem. Solids 69 (2008) 2548.
[15] M.H. Chan, W.Y. Ho, D.Y. Wang, F.H. Lu, 34th International Conference on Metallurgical Coatings and Thin Films, San Diego, CA, 2007, p. 962.
[16] D. Luca, D. Mardare, F. Iacomi, C.M. Teodorescu, International Workshop on Surface Physics, Polanica Zdroj, POLAND, 2005, p. 6122.
[17] A.L. Qu, X.F. Wen, P.H. Pi, J. Cheng, Z.R. Yang, Appl. Surf. Sci. 253 (2007) 9430.
[18] R.N. Wenzel, Ind. Eng. Chem. 28 (1936) 988.
[19] A.B.D. Cassie, S. Baxter, Trans. Faraday Soc. 40 (1944) 546.
[20] E. Bormashenko, R. Pogreb, T. Stein, G. Whyman, M. Erlich, A. Musin, V. Machavariani, D. Aurbach, Phys. Chem. Chem. Phys. 10 (2008) 4056.
[21] E. Bormashenko, T. Stein, R. Pogreb, D. Aurbach, J. Phys. Chem. C 113 (2009) 5568.
[22] A. Lafuma, D. Quere, Nat. Mater. 2 (2003) 457.
[23] Z. Yoshimitsu, A. Nakajima, T. Watanabe, K. Hashimoto, Langmuir 18 (2002) 5818.
[24] E. Bormashenko, R. Pogreb, G. Whyman, Y. Bormashenko, M. Erlich, Appl. Phys. Lett. 90 (2007).
[25] E. Bormashenko, R. Pogreb, G. Whyman, M. Erlich, Langmuir 23 (2007) 6501.
[26] E. Bormashenko, R. Pogreb, G. Whyman, M. Erlich, Langmuir 23 (2007) 12217.
[27] J.H. Lee, I.C. Leu, M.C. Hsu, Y.W. Chung, M.H. Hon, J. Phys. Chem. B 109 (2005) 13056.
[28] M.S. Sander, H. Gao, J. Am. Chem. Soc. 127 (2005) 12158.
[29] B.B. Lakshmi, P.K. Dorhout, C.R. Martin, Chem. Mater. 9 (1997) 857.
[30] M.Z. Yin, Y.J. Cheng, M.Y. Liu, J.S. Gutmann, K. Mullen, Angew. Chem. Int. Ed. 47 (2008) 8400.
[31] D. Chandra, A. Bhaumik, Microporous Mesoporous Mater. 112 (2008) 533.
[32] A. Mitra, A. Bhaumik, B.K. Paul, Microporous Mesoporous Mater. 109 (2008) 66.
[33] H. Weixin, H. Hong, L. Hui, Z. Zhihui, Mater. Res. Innovations 13 (2009) 253.
[34] Z.F. Liu, Z.G. Jin, W. Li, J.J. Qiu, Mater. Lett. 59 (2005) 3620.
[35] M. Miyauchi, H. Tokudome, J. Mater. Chem. 17 (2007) 2095.
[36] M. Nosonovsky, B. Bhushan, Mater. Sci. Eng., R 58 (2007) 162.
[37] E. Bormashenko, Colloids Surf., A 324 (2008) 47.